Available online at www.sciencedirect.com

ScienceDirect

Polar Science 8 (2014) 283–297

http://ees.elsevier.com/polar/

Seasonal variability of phytoplankton biomass and composition in the major water masses of the Indian Ocean sector of the Southern Ocean

Takahiro Iida [a,b,*], Tsuneo Odate [a,b]

[a] National Institute of Polar Research, 9-10 Midori-cho, Tachikawa, Tokyo 190-8518, Japan
[b] Department of Polar Science, School of Multidisciplinary Sciences, Graduate University for Advanced Studies, Kanagawa, Japan

Received 9 September 2013; revised 19 March 2014; accepted 31 March 2014
Available online 12 April 2014

Abstract

Long-term changes in phytoplankton biomass and community composition are important in the ecosystem and biogeochemical cycle in the Southern Ocean. We aim to ultimately evaluate changes in phytoplankton assemblages in this region on a decadal scale. However, yearly continuous data are lacking, and long-term datasets often include seasonal variability. We evaluated the seasonal changes in phytoplankton abundance/composition across latitudes in the Indian Ocean sector of the Southern Ocean via multi-ship observations along the 110°E meridian from 2011 to 2013. The chlorophyll *a* concentration was 0.3–0.5 mg m^{-3} in the Subantarctic Zone (40–50°S) and 0.4–0.6 mg m^{-3} in the Polar Frontal Zone (50–60°S); pico-sized phytoplankton (<10 μm), mainly haptophytes, were dominant in both zones. In the Antarctic Divergence area (60–65°S), the chlorophyll *a* concentration was 0.6–0.8 mg m^{-3}, and nano-sized phytoplankton (>10 μm), mainly diatoms, dominated. Chlorophyll *a* concentrations and phytoplankton community compositions were the same within a latitudinal zone at different times, except during a small but distinct spring bloom that occurred north of 45°S and south of 60°S. This small seasonal variation means that this part of the Southern Ocean is an ideal site to monitor the long-term effects of climate change.

Keywords: Phytoplankton; Size fraction; Seasonal variability; Pigment analysis; CHEMTAX

1. Introduction

The Southern Ocean is very important to the global carbon cycle. One reason is that it occupies approximately 20% of the world's ocean area, and another is its very high primary productivity (Arrigo et al., 1998a). This area is a critical CO_2 sink globally, with the region south of 50°S accounting for about 20% of the global ocean CO_2 sink (Takahashi et al., 2009). Its carbon absorption rate is approximately 1.5×10^{15} g C yr^{-1} (McNeil et al., 2007).

The Southern Ocean is also one of the largest high-nutrient low-chlorophyll (HNLC) areas. Iron availability may control the biomass and productivity of phytoplankton (Martin et al., 1990). However,

* Corresponding author. National Institute of Polar Research, 9-10 Midori-cho, Tachikawa, Tokyo 190-8518, Japan. Tel.: +81 42 512 0742; fax: +81 42 528 3492.
E-mail addresses: iida@nipr.ac.jp (T. Iida), odate@nipr.ac.jp (T. Odate).

http://dx.doi.org/10.1016/j.polar.2014.03.003
1873-9652/

phytoplankton blooms often have been observed in several regions near fronts and in sea ice retreat areas (Comiso et al., 1993; Moore and Abbott, 2000). Large phytoplankton blooms transport particulate organic carbon in the frustules of diatoms from the surface layer of deep oceans. Diatoms are the main component of the phytoplankton community in blooms around fronts (Brzezinski et al., 2001); therefore, diatom blooms are very important for carbon cycling in these areas. Diatom blooms mainly occur in polar front areas, while blooms in seasonal ice areas are dominated by non-calcifying haptophytes, e.g. *Phaeocystis antarctica* (Arrigo et al., 1998b). Large carbon exports occur in haptophyte bloom areas as well (DiTullio et al., 2000). Therefore, phytoplankton blooms and variability in their compositions affect the carbon cycle in the Southern Ocean.

The Southern Ocean also has one of the highest biological productivities in the world. In particular, the Antarctic krill *Euphausia superba* is a key species in this area, and most of the sea mammals, sea birds, and fishes depend on it for survival (e.g. Hempel, 1985). Consequently, the biomass of phytoplankton, the food source for krill, is an important factor in this ecosystem, and changes in primary productivity have large effects on the community and the carbon cycle in this region.

The most unique hydrographic feature in the Southern Ocean is the circumpolar current, which strongly affects the global carbon cycle and ecosystem dynamics. The Antarctic Circumpolar Current (ACC), a major current in the Southern Ocean, is induced by strong westerly winds between 45°S and 55°S (Nowlin and Klinck, 1986). The ACC flows through the Atlantic, Indian, and Pacific oceans without continental barriers. Therefore, the ACC is the most important factor affecting biogeochemical cycles, including the iron cycle, in the Southern Ocean (e.g. Nowlin and Klinck, 1986; Tynan, 1998; Boyd and Ellwood, 2010). The ACC is also associated with several oceanic fronts: the Subtropical Front (STF), the Subantarctic Front (SAF), the Polar Front (PF), the Southern ACC Front (SACCF), and the Southern Boundary (SB) of the ACC (Orsi et al., 1995; Belkin and Gordon, 1996). These frontal regions are characterized by sharp horizontal gradients in hydrographic properties that represent the boundaries of distinct water masses (Orsi et al., 1995; Belkin and Gordon, 1996; Rintoul and Bullister, 1999; Sokolov and Rintoul, 2002).

Seasonal sea ice cover also affects phytoplankton dynamics in the Southern Ocean. The sea ice is distributed zonally by latitude, and it affects the habitats of phytoplankton and zooplankton in these areas (Massom and Stammerjohn, 2010). Antarctic zooplankton communities can be divided into three ice-associated zones: 1) the permanent ice-free area, dominated by copepods and salps; 2) the seasonal sea ice zone, dominated by *E. superba*; and 3) the permanent sea ice area, dominated by ice krill (*Euphausia crystallorophias*) (Loeb, 2007). The distributions of phytoplankton communities are closely related to these fronts and to the distribution of sea ice.

Interannual variations in phytoplankton distribution and primary productivity affect ecosystems and carbon cycles in the Southern Ocean. The changes in carbon cycling in the Southern Ocean can have global effects because of thermodynamic circulation. Several studies have examined the variations in phytoplankton distribution and primary productivity in the Indian Sector of the Southern Ocean (e.g. Strutton et al., 2000; Wright et al., 2010). In particular, Johnston and Gabric (2010) revealed that the Southern Annual Mode (SAM) and sea surface temperatures (SST) produced conditions that were favorable for phytoplankton growth, based on analyses of satellite remote sensing datasets. Interannual variations in annual productivity were most closely linked to changes in sea ice cover, although sea surface temperature also played a role, and only 31% of the variation in annual production was explained by the SAM.

Annual primary production could increase in the future as stronger winds increase nutrient upwelling (Arrigo et al., 2008). However, although the satellite chlorophyll (chl) *a* dataset has been available since 1996, continuous datasets based on direct observations are scarce for the Southern Ocean. The only monitoring station datasets were collected in the Antarctic Peninsula region (Montes-Hugo et al., 2009), and very limited data are available for other areas of the Southern Ocean. The Japanese Antarctic Research Expedition (JARE) has conducted monitoring since 1965 in the Indian Ocean Sector of Southern Ocean using the icebreakers *Fuji* (1965–1983) and *Shirase* (1983–present) to discover long-term trends in the oceanic environment. All hydrographic and biological data have been published by the National Institute of Polar Research (NIPR) (http://ci.nii.ac.jp/vol_issue/nels/AA10457766_en.html). However, because these data were sometime collected in different seasons and at different positions and depths, long-term variations in primary productivity are difficult to evaluate directly. Therefore, we must identify seasonal changes in phytoplankton distribution and composition before

we can evaluate the interannual variations in phytoplankton based on spasmodic observation datasets.

At two time points during the austral summer from 2011 to 2013, time-series observations were conducted in the Eastern Indian Ocean sector of the Southern Ocean during cruises by several Japanese research vessels. The sampling stations were distributed from the permanently ice-free area to the seasonally ice-covered area. The ultimate goal of this study is to clarify the long-term variability of phytoplankton biomass and composition in the Indian Ocean sector of the Southern Ocean. First, we must study the seasonal variations in hydrography and pigment-based phytoplankton assemblages in these areas with the aim of evaluating the factors controlling these changes.

2. Methodology

2.1. Time-series in situ multi-ship observations

Time-series hydrographic observations were conducted during cruises of the ice-breaker *Shirase* (Japanese Marine Self Defense Force) and TRV *Umitaka-Maru* (Tokyo University of Marine Science and Technology) along the 110°E meridian from 40°S to 66°S in the Indian sector of the Southern Ocean in the austral spring and summer of 2011/2012 and 2012/2013 (Fig. 1). Additional data were collected during the cruise of *Shirase* in December 2011, March 2012, and December 2012, and during cruises of *Umitaka-Maru* in January 2011, 2012, and 2013. The five hydrographic stations were located along the 110°E meridian (at intervals of 5° latitude for both ships). These observations were conducted as part of the JARE long-term oceanographic monitoring program, supported by the Ministry of Education, Culture, Sports, Science and Technology (MEXT), Japan. On the *Shirase*, vertical profiles of temperature and salinity were collected using a conductivity–temperature–depth (CTD) probe (SBE 19 plus; Sea-Bird Electronics, Bellevue, WA, USA) with a water sampler (SBE 55 ECO, Sea-Bird Electronics) to depths of 500 m. On the *Umitaka-Maru*, these data were collected by an SBE 9 plus with a 24 Niskin bottle water sampler (SBE 35, Sea-Bird Electronics) to the depth of the sea floor. The CTD sensors were calibrated before each cruise. Seawater samples from deeper than 10 m were collected using 4-L (*Shirase*) and 2.5-L (*Umitaka-Maru*) Niskin bottles at predefined depths of 20, 50, 75, and 100 m and of 10, 20, 30, 50, 75, and 100 m, respectively. Surface waters were sampled for phytoplankton analysis 2–4 times per day along the ship transects in each cruise (Fig. 1). Seawater was pumped from an inlet at the bottom of the ship (about 8 m below sea level for the *Shirase*, and 4 m below sea level for the *Umitaka-Maru*) with a coated titanium pipe. Furthermore, the sea surface temperature and salinity were monitored continuously at 10-s intervals on both vessels. The temperature sensor (SBE 38, Sea-Bird Electronics) was located close to the inlet pipe at the bottom of the ship. The salinity sensor was located in the ship laboratory.

2.2. Phytoplankton pigment analysis

Water samples for phytoplankton analyses were kept in dark bottles during both cruises. To measure chl *a* concentrations, samples were filtered with positive pressure (<0.01 MPa) through two Nuclepore filters with pore sizes of 2 μm and 10 μm. The filtrate was refiltered onto glass fiber Whatman GF/F filters to obtain phytoplankton cells less than 2 μm and 10 μm. The filters were immediately soaked in N,N-dimethylformamide (Suzuki and Ishimaru, 1990), and pigments were extracted on board. The concentration of chl *a* was determined with a fluorometer (10-AU, Turner Designs, Sunnyside, CA, USA) (Parsons et al., 1984). We used the Welschmeyer method to measure chl *a* (Welschmeyer, 1994). The fluorometer was calibrated against a chl *a* standard (Wako Chemicals, Osaka, Japan) using a spectrophotometer before each cruise. The value of the specific absorption coefficient reported by Porra et al. (1989) was used in calculations.

Water samples (1.0–4.0 L) for HPLC pigment analysis were filtered with positive pressure (<0.01 MPa) on board onto 25-mm Whatman GF/F filters. The filters were immediately frozen in liquid nitrogen and stored at −80 °C until analysis. Before HPLC analysis, the filters were cut into small pieces, soaked in 3 ml N,N-dimethylformamide containing canthaxanthin solution (Wako Chemicals) as an internal standard, and then sonicated for 30 s to break the cell walls. Debris and glass fibers were removed by filtering the samples through 0.4-μm polytetrafluoroethylene membrane filters. After extraction, pigments were separated and quantified with a Prominence HPLC System (Shimadzu, Kyoto, Japan) as described by Van Heukelem and Thomas (2001) (the VHT method). We slightly modified the gradient system to clearly separate pigments (Table 1). Before analyses, the HPLC was calibrated with commercially available pigment standards. We used chl *a*, chl *b*, lutein, zeaxanthin (Extrasynthese), chlorophyll cl, chlorophyll c2,

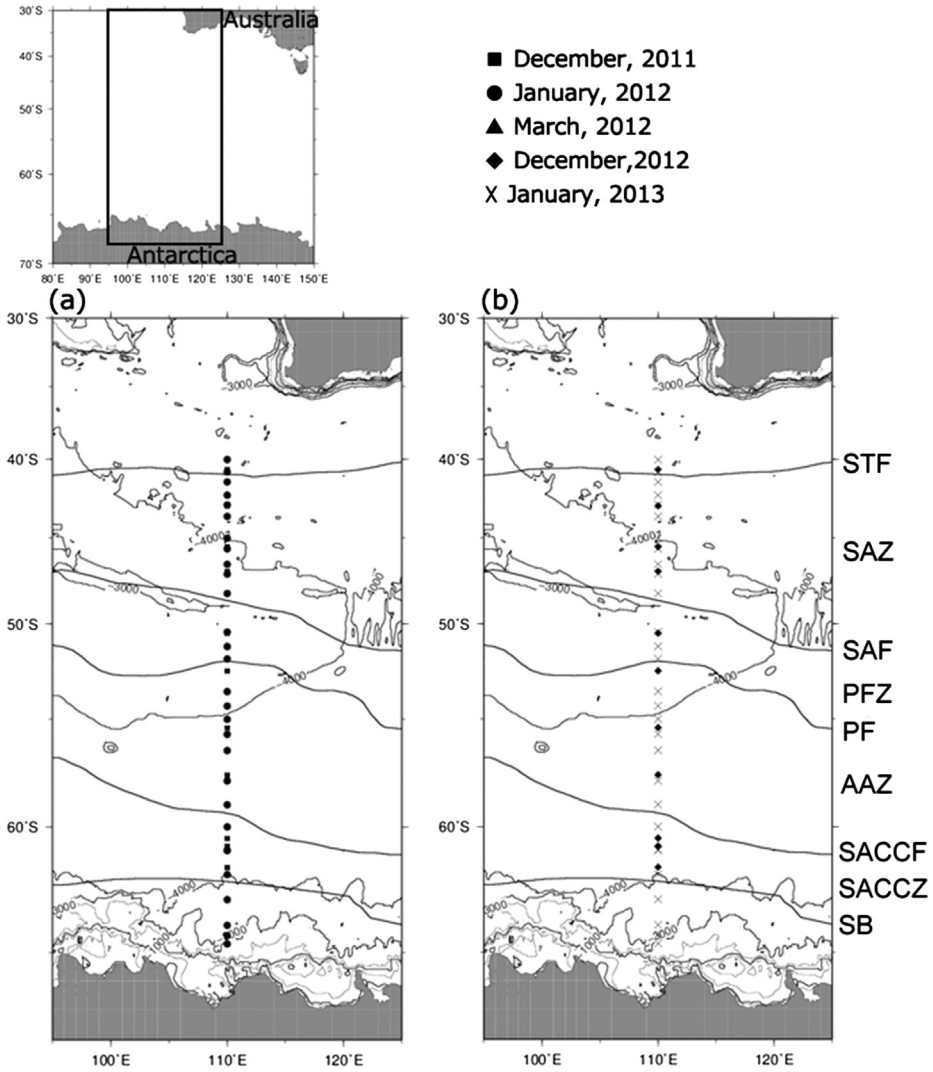

Fig. 1. Cruise transect along the 110°E meridian in the Indian sector of the Southern Ocean. Lines show climatological locations of the five fronts (Orsi et al., 1995) (a: 2011/2012 season, b: 2012/2013 season observation stations). STF, Subtropical Front; SAF, Subantarctic Front; PF, Polar Front; SACCF, Southern Antarctic Circumpolar Current Front; SB, Southern Boundary; SAZ, Subantarctic Frontal Zone; PFZ, Polar Frontal Zone; AAZ, Antarctic Zone; SACCZ, Southern ACC (Antarctic Circumpolar Current) Frontal Zone.

peridinin, fucoxanthin, 19′-hexanoyloxyfucoxanthin, alloxanthin, prasinoxanthin, diadinoxanthin as the standards. All pigments were provided by the Danish Hydraulic Institute [DHI] Water & Environment, Denmark. Pigments separated by HPLC were identified by comparing their retention times and absorbance spectra with those of the standards.

2.3. CHEMTAX analysis

We used CHEMTAX methodology to identify the dominant phytoplankton species (Mackey et al., 1996). CHEMTAX analysis provides data about each phytoplankton class in terms of its contribution to total chl *a* biomass based on HPLC pigment analyses. An initial ratio of the calculation matrix was determined as described by Mackey et al., 1996 (Table 2a). In the CHEMTAX analysis, the phytoplankton were separated into eight community types: cyanobacteria, dinoflagellates, chlorophytes, prasinophytes, cryptophytes, haptophytes types 3 and 4, and diatoms. This separation was based on previous phytoplankton community studies in the Southern Ocean. In our study, the haptophyte group was divided into two types (T3 and T4) because of large differences in pigment compositions between the calcified *Emiliania huxleyi*

Table 1
Gradient system used in VHT method.

Step	Time	A (%)	B (%)
Start	0	95	5
2	25	35	65
3	31	5	95
End	42	95	5

Solvent A, 70:30 methanol: 28 mM aqueous TBAA, pH 6.4.
Solvent B, 100% methanol.

and the non-calcified *Phaeocystis antarctica* (Jeffrey and Wright, 1994). These species are commonly distributed in the Southern Ocean and cause large blooms in the seasonal sea ice area (Iida et al., 2012; Arrigo et al., 1998b).

CHEMTAX analyses were conducted using the procedures described in Latasa (2007) with CHEMTAX version 1.95 (pers. comm. with S. Wright). CHEMTAX was run using the following parameters: ratio-limits = 500, initial time step = 10, step ratio = 1.03, epsilon limit = 0.0001, cut-off step = 30,00,000, iterations limit = 250, elements varied = 14 (number of pigments), subiterations = 1, weighting = bound relative (20) (Latasa et al., 2010). The final pigment ratio matrix obtained from CHEMTAX calculations varied slightly from the initial ratio. However, these variations were within the acceptable range proposed by Mackey et al. (1996); therefore, our initial assumptions were considered to be reasonable.

2.4. Light microscopy analysis

To verify the results of the CHEMTAX phytoplankton composition analysis, we evaluated the phytoplankton composition in water samples under a light microscope. For these analyses, 500-mL seawater samples from pumped surface waters were evaluated. The water samples preserved with 4% Lugol's iodine solution were kept in a refrigerator until analysis. Phytoplankton cells were identified and counted on land. Quantitative analyses were difficult because of the low cell abundance (except for diatoms).

3. Results

3.1. Seasonal changes in hydrographic structure and chl a

The vertical profiles of temperature showed significant seasonal variability along the 110°E meridian, but salinity did not show seasonal trends (Fig. 2). The spatial sampling interval was too long to observe details of the fronts, but some water masses could be identified in this area. A strong frontal structure was observed in the upper 500 m between 45°S and 50°S, corresponding with the SAF fronts in December and March, which coincided with the main stream of the ACC. There were broad distances between isothermal lines in January because of surface heating.

Table 2
Pigment: Chl *a* ratio used in CHEMTAX calculations, showing initial (a) and final ratio matrices (b).

Class	Chl c_3	Peri	19′ but	Fuco	Neo	Pras	Viola	19′ Hex	Diad	Allox	Lutein	Zeax	Chl *b*
(a) Initial ratios													
Diat	0	0	0	0.76	0	0	0	0	0.14	0	0	0	0
Hapt(T3)	0.05	0	0	0	0	0	0	1.71	0.14	0	0	0	0
Hapt(T4)	0.05	0	0.25	0.58	0	0	0	0.54	0.12	0	0	0	0
Cryp	0	0	0	0	0	0	0	0	0	0.23	0	0	0
Pras	0	0	0	0	0.15	0.32	0.06	0	0	0	0.01	0	0.95
Chlo	0	0	0	0	0.06	0	0.06	0	0	0	0.20	0	0.26
Dino	0	1.06	0	0	0	0	0	0	0	0	0	0	0
Cyan	0	0	0	0	0	0	0	0	0	0	0	0.35	0
(b) Final ratios													
Diat	0	0	0	0.30	0	0	0	0	0.09	0	0	0	0
Hapt(T3)	0.02	0	0	0	0	0	0	0.59	0.05	0	0	0	0
Hapt(T4)	0.11	0	0.08	0.09	0	0	0	0.19	0.07	0	0	0	0
Cryp	0	0	0	0	0	0	0	0	0	0.19	0	0	0
Pras	0	0	0	0	0.06	0.03	0.03	0	0	0	0.00	0	0.45
Chlo	0	0	0	0	0.04	0	0.04	0	0	0	0.13	0	0.16
Dino	0	0.51	0	0	0	0	0	0	0	0	0	0	0
Cyan	0	0	0	0	0	0	0	0	0	0	0	0.37	0

Abbreviations: Diat = Diatom; Hapt(T3) = haptophytes (Type 3: *Emiliania huxleyi*); Hapt(T4) = haptophytes (Type 4: *Phaeocystis antarctica*); Cryp = cryptophytes; Pras = prasinophytes; Chlo = chlorophytes; Dino = dinoflagellates; Cyan = cyanobacteria.

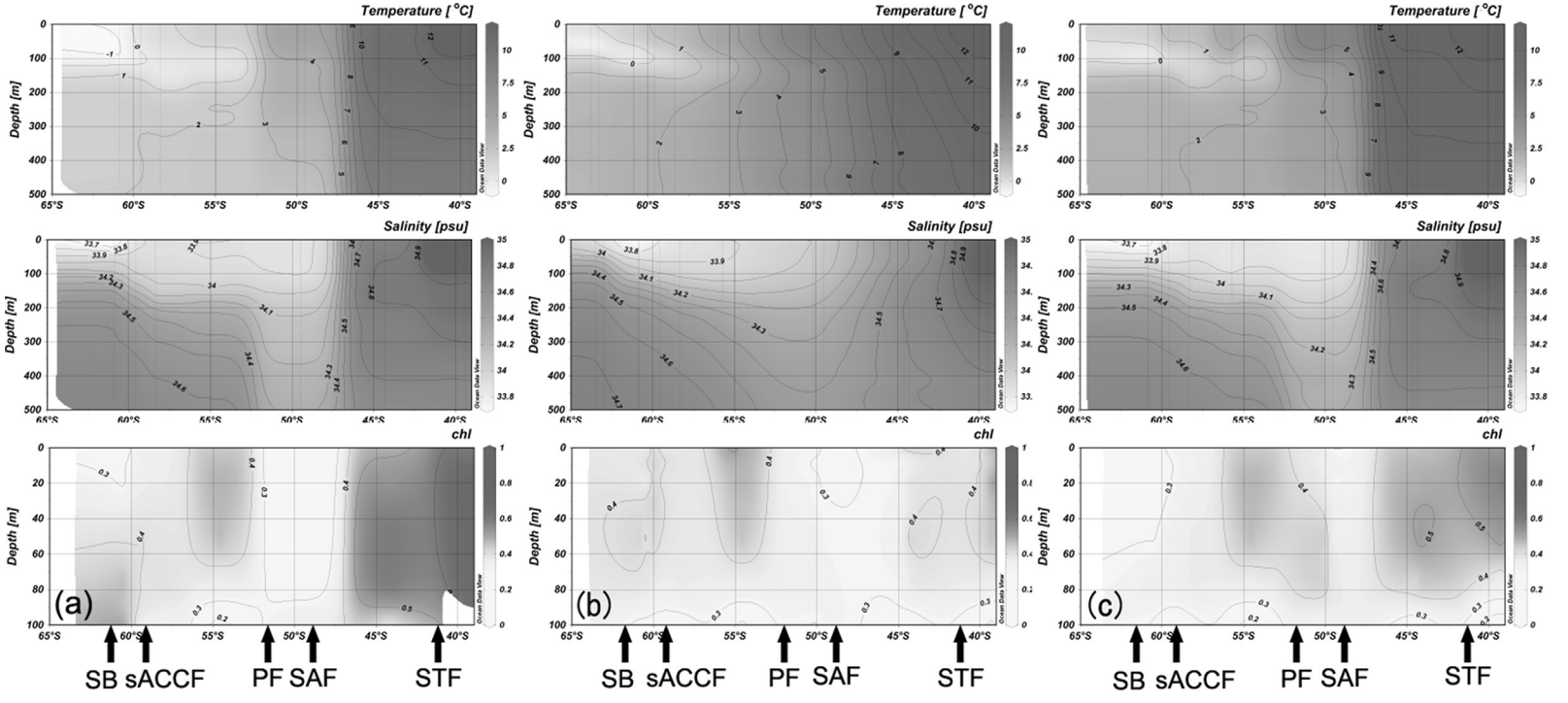

Fig. 2. Vertical distributions of temperature, salinity, and chlorophyll *a* concentrations in the upper 100 m of the water column during 2011/2012 (a: December, 2011, b: January, 2012, c: March, 2012). Arrows indicate front positions suggested by Orsi et al. (1995).

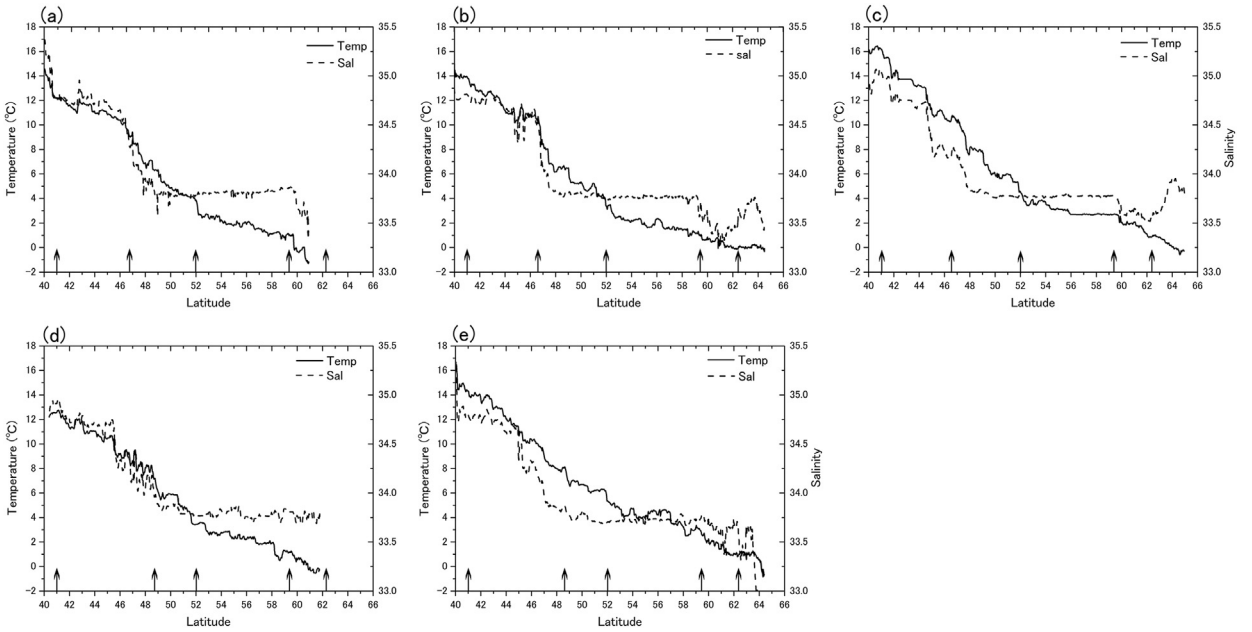

Fig. 3. Profiles of sea surface temperature and salinity in December, 2011 (a); January, 2012 (b); March, 2012 (c); December, 2012 (d); and January, 2013 (e). Arrows indicate front positions suggested by Orsi et al. (1995). STF, SAF, PF, SACCF and SB are as defined in the caption to Fig. 1 and located at 41°S, 48.7°S, 52.1°S, 59.4°S, and 62.3°S respectively along the 110°E meridian.

The PF marks the northern limit of the Antarctic Zone (Gordon et al., 1977) and is defined by the northernmost extent of the subsurface temperature minimum layer cooler than 2 °C. This minimum temperature layer is winter water found only south of the PF, and it occupies the water column between 100 and 300 m (Sokolov and Rintoul, 2007). This PF structure showed small seasonal variations (Fig. 2); water with the minimum subsurface temperature was located around 53°S, almost corresponding with the location estimated by Orsi et al. (1995). The SACCF is defined as the southernmost extent of water warmer than 1.8 °C in the maximum temperature layer (Orsi et al., 1995). The SACCF was identified around 60°S in our observations. The seasonal variability of the SACCF was small, like that of the PF. The Southern Boundary of the ACC and Antarctic Slope Front (ASF) are defined by the southern limit of the UCDW, which is observed as an oxygen minimum (Orsi et al., 1995). This coincides with the southern limit of water with a temperature maximum layer warmer than 1.5 °C in the Indian Sector of Southern Ocean (Sokolov and Rintoul, 2007). A water mass consistent with this definition was found between 62°S and 63°S in this study, and its seasonal variability was limited like those of the PF and SACCF. Therefore, clear seasonal variations in frontal structure were only observed for the SAF in this area.

The other regions south of the SAF showed only small seasonal variations in front structure and current systems. Our vertical observations were conducted at 5° latitude intervals, so detailed frontal structure information was limited. Therefore, we analyzed the surface T-S datasets collected on five cruises (Fig. 3). These data indicated that the temperature was warmer in January, however, the front areas were not consistent across years. Each of the fronts (SAF, PF, SACCF, and ASF) can be identified using surface temperature and salinity data. The temperature and salinity drop rapidly in the SAF (located at 48°S). The position of the SAF was the same as that predicted from vertical observations. The temperature and salinity changed gradually along the southern transect and corresponded with the locations of the PF (52°S), SACCF (60°S), and SAF (63°S).

Generally, phytoplankton blooms occur in spring in sub-polar regions. However, the chl *a* distribution along the 110°E meridian showed only very small seasonal changes (Fig. 2). There were higher chl *a* concentrations in the northern- and southern-most sections. The highest chl *a* concentrations were observed in the STZ in December (about 1.3 mg m^{-3}) and in the Antarctic Zone (AAZ) in January (about 1.0 mg m^{-3}), moderate concentrations were observed in the Polar Frontal Zone (PFZ) (about 0.3–0.5 mg m^{-3}), and the lowest chl *a* concentrations

were recorded in the Subantarctic Zone (SAZ) (<0.3 mg m^{-3}).

3.2. Seasonal changes in surface phytoplankton composition

A sub-surface chl *a* maximum (SCM) was often observed in the Southern Ocean. However, the SCM was difficult to identify clearly along most of the 110°E meridian without knowing the positions of the SB in December 2011 and at the PF in March 2012 (Fig. 2). Surface chl *a* concentrations are more useful for long-term monitoring because of the ease of regular collection and for comparing with satellite data, so we examined surface chl *a* (bulk- and size-fractioned) distribution in this area (Fig. 4). We compared the 2011/2012 and 2012/2013 seasons to investigate the interannual variability of phytoplankton distributions. The highest chl *a* concentration was in the southern region, especially south of the SACCF in each month/year (approximately south of 61°S). In December, 2012, there were patchy regions of high chl *a* concentrations around some fronts (47°S and 55.5°S). The relative contributions of size-fractionated cell chl *a* to total chl *a* at surface stations is shown in Fig. 4. Micro-sized cells (>10 μm) were dominant and the relative abundance of these cells increased at the southern stations (approximately south of 61°S). In other regions, pico-sized cells (0.7–2 μm) and nano-sized cells (2–10 μm) were generally more abundant, except in the patchy regions with high chl *a* concentrations (December, 2012, 47°S and 55.5°S).

We also used CHEMTAX analyses to evaluate phytoplankton composition based on algal pigment data (Fig. 5). In early December, cyanobacteria contributed 40% of total chl *a* in the STF area. In the area between the SAF and SACCF (50–60°S), haptophytes (60–70%) and diatoms (20–30%) dominated the surface layer. At most of the southern stations, diatoms were dominant (60–70%), and the contribution of each of the other groups decreased by approximately 10%. In January, cyanobacteria disappeared from the STF area, whereas the contribution of haptophytes increased to 30%. Haptophytes were dominant in the PF area, and diatoms made the highest contribution to total chl *a* in the area south of the SACCF in December. In March, the proportion of cyanobacteria increased again in the STF, but the dominant group was the haptophytes. The haptophytes were also dominant in the PF area, and the ratio of

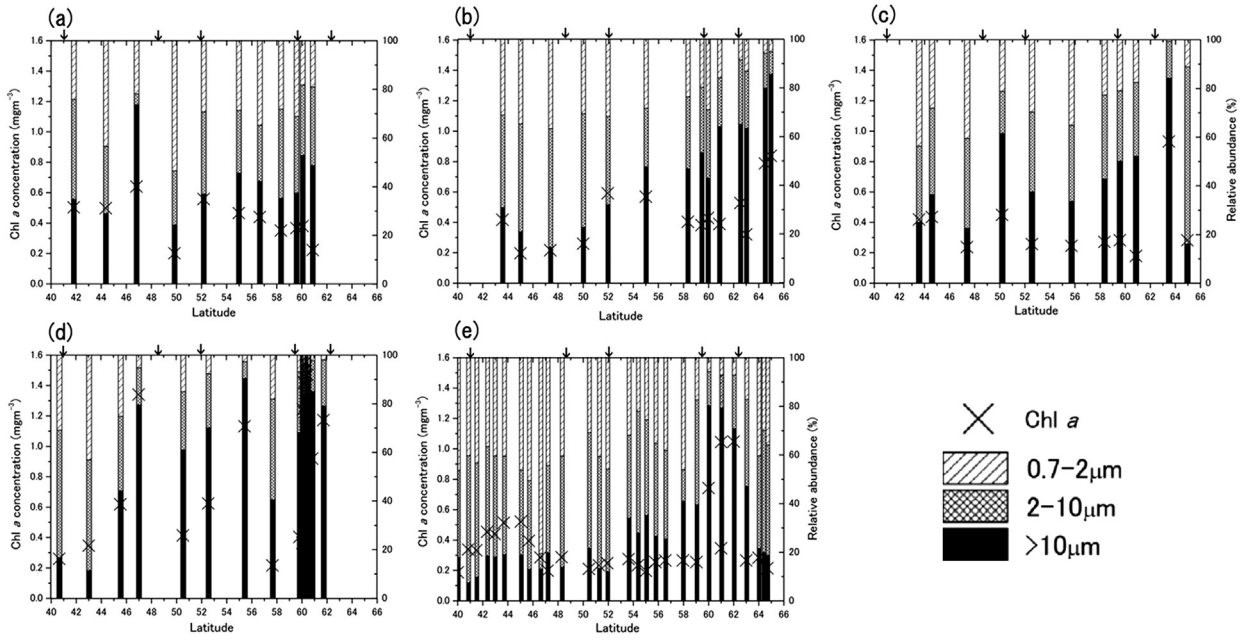

Fig. 4. Relative abundance of phytoplankton in each size class in surface seawater samples, and proportion of chlorophyll *a* (to total chlorophyll *a*) attributed to each size class. Sea surface water samples were collected along the 110°E meridian in December, 2011 (a), January, 2012 (b), March, 2012 (c), December, 2012 (d), and January, 2013 (e). Arrows indicate front positions suggested by Orsi et al. (1995). STF, SAF, PF, SACCF and SB are as defined in the caption to Fig. 1 and located at 41°S, 48.7°S, 52.1°S, 59.4°S, and 62.3°S respectively along the 110°E meridian.

diatoms increased at the more southern stations. Prasinophytes were only found in the STF area, where they contributed less than 10% of total chl *a*. Dinoflagellates and cryptophytes were commonly found in every area and season, however, their contribution to total chl *a* (<10%) was smaller than those of the other phytoplankton groups.

3.3. Time series of chl a concentrations derived from ocean color remote sensing

There were greater differences in chl *a* concentrations and phytoplankton species compositions among latitudinal zones than among seasons. However, the variations were observed only three (or two) times per year. The surface and subsurface chl *a* concentrations were relatively uniform in our on-board analyses. Therefore, we analyzed ocean color remote sensing datasets to evaluate spatial variability in detail, especially in frontal areas (Fig. 6). A time-series of surface chl *a* data from January 2011 to March 2013 was constructed using MODIS (MODerate resolution Imaging Spectroradiometer) data downloaded from the ocean color web (http://oceancolor.gsfc.nasa.gov). We used the MODIS level 3 daily standard mapped image 9-km resolution data for temporal analysis. We extracted chl *a* data, which were calculated using the NASA standard algorithm (OC3Mv6) (O'Reilly et al., 2000). Ocean color data cannot be observed under clouds; therefore, we extracted and averaged the available cloud-free data with 5 × 5 pixel resolution (45 km × 45 km). The data points were spaced at approximately 0.5° latitudinal intervals between 40°S and 66°S. High chl *a* concentrations were found south of 60°S. This region was covered by sea ice from May to October (e.g. Massom et al., 2013). Generally, melting of sea ice drives phytoplankton blooms. However, no clear blooming events occurred in this region. Another distinctive feature was the seasonal variation in the SAZ. There were relatively high chl *a* concentrations from January to March compared with those in other months. There was a very low chl *a* concentration (<0.2 mg m^{-3}) around the PFZ. Overall, the seasonal variations in the chl *a* concentration were small, except during a distinct spring bloom along the 110°E meridian in the Indian Ocean sector of the Southern Ocean. The chl *a* concentrations and phytoplankton species compositions differed among the frontal zones (SAZ, PFZ, AAZ, and the Southern ACC Frontal Zone (SACCZ)).

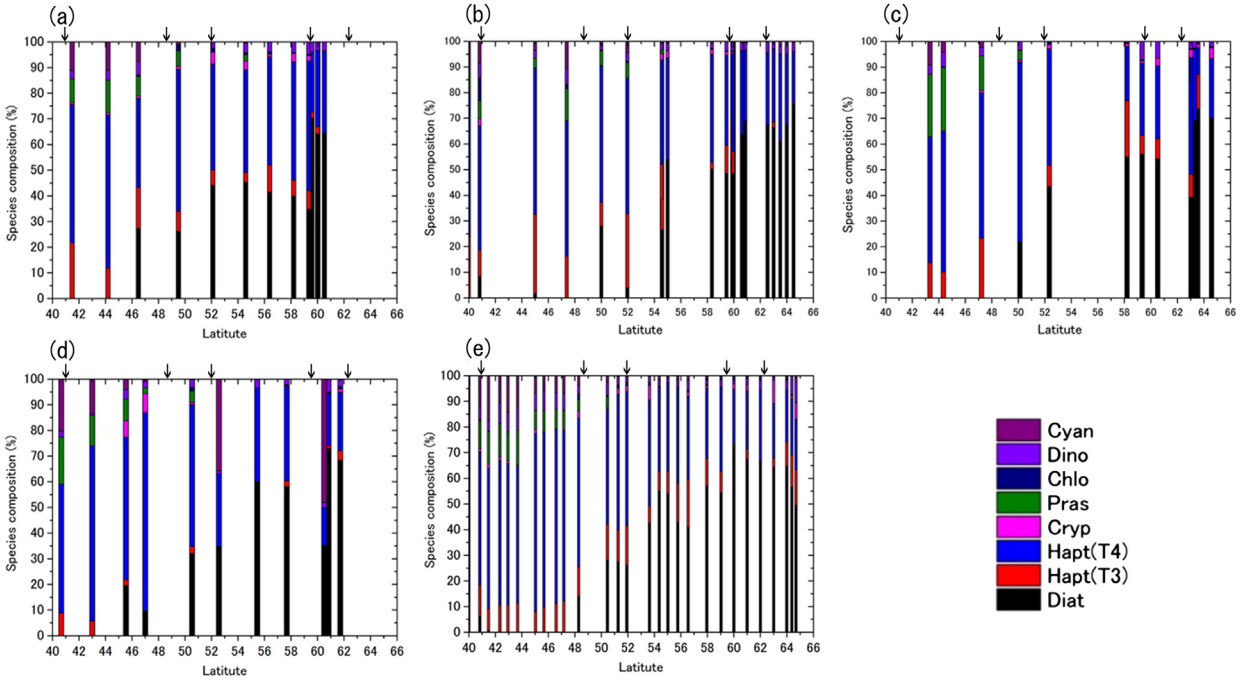

Fig. 5. Relative composition of phytoplankton in the surface water along 110°E meridian based on CHEMTAX analyses of pigment data. December 2011 (a), January 2012 (b), March 2012 (c), December 2012 (d), January 2013 (e). Arrows indicate front positions suggested by Orsi et al. (1995). STF, SAF, PF, SACCF and SB are as defined in the caption to Fig. 1 and located at 41°S, 48.7°S, 52.1°S, 59.4°S and 62.3°S respectively along the 110°E meridian.

3.4. Nutrient distribution derived by WOCE

The phytoplankton composition showed analogous patterns in same latitudinal zone (Fig. 5). The nutrient concentrations should affect phytoplankton composition. Unfortunately, we do not have enough nutrient samples from these cruises and cannot show the vertical distributions of nutrients. Therefore, we analyzed World Ocean Circulation Experiment (WOCE) datasets. During the WOCE Southern Ocean cruises by the RSV *Aurora Australis* in the 2004/2005 austral summer season, the nutrient distribution was investigated along the 115°E meridian (Tilbrook et al., 2001). The vertical sections of nitrate, phosphate, and silicate concentrations along the 115°E transect are shown in Fig. 7. All of the nutrients showed higher concentrations at the southern stations. However, the ratio of change in concentration differed among the nutrients. In particular, nitrate and phosphate remained at higher levels while silicate was present at extremely low concentrations (<10 μg m^{-3}) in the northern regions. These distributions would be important for phytoplankton compositions in the Indian Sector of the Southern Ocean.

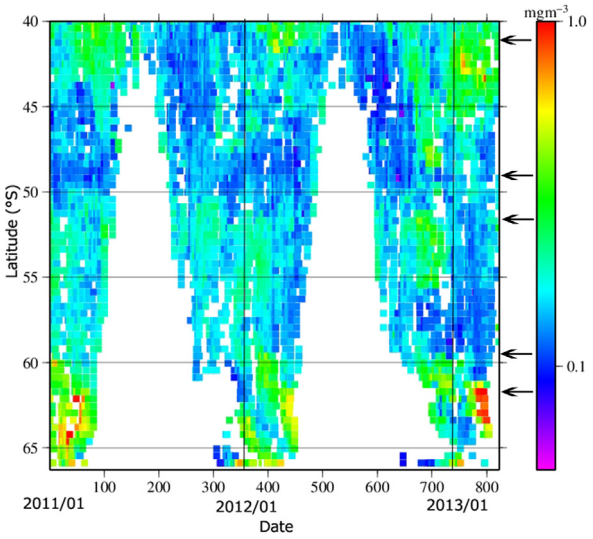

Fig. 6. Temporal and spatial variability of satellite-derived chlorophyll *a* concentrations along the 110°E meridian. Data points were extracted from 5 × 5 pixels (=45 km × 45 km) from MODIS level 3 daily standard mapped images. Arrows indicate front positions suggested by Orsi et al. (1995). STF, SAF, PF, SACCF and SB are as defined in the caption to Fig. 1 and located at 41°S, 48.7°S, 52.1°S, 59.4°S and 62.3°S respectively along the 110°E meridian.

4. Discussion

4.1. Phytoplankton blooms and hydrography

The results of our study show the characteristics of seasonal variations in chl *a* concentrations and phytoplankton compositions in the Indian Ocean sector of the Southern Ocean. The phytoplankton composition was uniform within the same latitudinal zone at different times. However, small but distinct spring blooms were detected in the SAZ and SACCZ. Previous studies revealed that the diatom *Fragilariopsis kerguelensis* bloomed around the Kerguelen Plateau and that it showed regional and seasonal variations in its abundance (Blain et al., 2007; Mongin et al., 2008). We detected a small bloom around the 110°E meridian, an area downstream of the ACC from the Kerguelen Plateau. The mechanisms of high productivity in the Kerguelen Islands have been already investigated. The strong ACC strikes against the Kerguelen Plateau, one of the largest continental shelves in the world, results in a large amount of natural iron fertilization as a result of sub-surface water upwelling (Blain et al., 2008). This water mass advects onto some pathways downstream of the ACC with many eddies and meanders. The water mass containing high phytoplankton biomass advected westerly, but the phytoplankton mass disappeared around 90°E because of iron limitation. Thus, the water mass at the 110°E meridian isn't affected by variations at the Kerguelen Plateau.

Sokolov and Rintoul (2007) suggested that there was little evidence that the fronts of the ACC are associated with enhanced productivity. Rather, for most regions with elevated chl *a* levels in the open Southern Ocean, the higher productivity can be explained by the upwelling of nutrients where the ACC interacts with topography, followed by downstream advection. Our study showed similar results, and we observed that the phytoplankton composition was the same within the same latitudinal zone. Johnston and Gabric (2011) investigated latitude zonal mean values of chl *a* concentration in the Indian Ocean sector of the Southern Ocean (110–160°E, 40–70°E) using satellite data. They found that the zonal mean chl *a* value showed small seasonal variations, except in the area south of 65°S. The high interannual variability in that area was due to the retreat of sea ice. These results were almost same as those in our study, except for the most southern station.

Next, we considered whether currents upstream of the ACC from the Kerguelen Islands could explain our findings. In a previous study, the highest pigment concentrations were detected between the fronts, rather than in the current cores in the Atlantic Sector of the

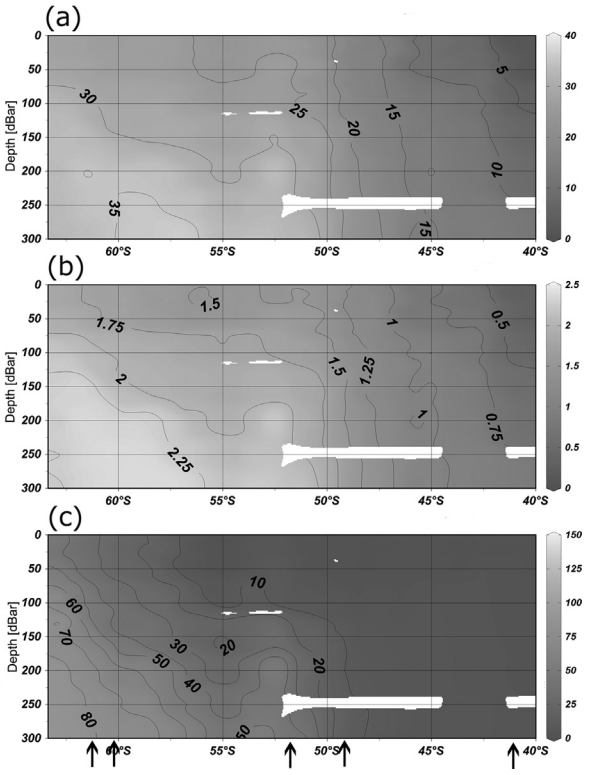

Fig. 7. Vertical distributions of nitrate (a), phosphate (b), and silicate (c) concentrations in upper 200 m of the water column along the 115°E meridian (collected during WOCE cruise). Arrows indicate front positions suggested by Orsi et al. (1995). STF, SAF, PF, SACCF and SB are as defined in the caption to Fig. 1 and located at 41°S, 49.4°S, 52.6°S, 60.5°S and 62.5°S respectively along the 115°E meridian.

Southern Ocean (Veth et al., 1997). Furthermore, the distributions of phytoplankton pigments also reflected the structure of the fronts, with distinct phytoplankton communities detected between fronts (Bathmann et al., 1997; Peeken, 1997). Phytoplankton blooms dominated by diatoms, mainly *F. kerguelensis*, have been observed in the PFZ. Other groups contributing to the phytoplankton biomass included prymnesiophytes, green algae, dinoflagellates, and cryptophytes; the distributions of these groups varied over time (Peeken, 1997). We found that diatoms were not the dominant species in the PFZ at 110 E. The reasons for the differences between our results and those of other studies are discussed later in this paper.

Overall, the phytoplankton variability along the 110°E meridian should be affected by the amount of iron fertilization from the sub-surface water mass. If the ACC has become stronger because of strong westerly winds, then meanders and eddies will be induced around the Kerguelen Plateau. On the other hand, there are few meanders and eddies downstream of the Kerguelen Plateau, a typical high-nutrient low-Chl *a* (HNLC) region, where phytoplankton primary productivity is affected by iron fertilization from vertical mixing or from dust. The ocean region south of Australia is far from the continent and receives little dust (Li et al., 2008). Therefore, wind mixing should be the main cause of iron fertilization in the study area. Recently, it was reported that westerly winds are becoming much stronger as a result of climate change (e.g. Toggweiler and Russell, 2008). The strong westerly winds should enhance iron fertilization; however, the mechanism is likely to be complicated because of the combination of vertical and horizontal mixing. On the other hand, only vertical wind mixing affects surface iron fertilization along the 110°E meridian, making the effects of climate change on phytoplankton in this environment easy to evaluate. In other words, the current phytoplankton distribution could be considered as "background values" to evaluate the changes in the marine environment and ecosystems resulting from climate change and global warming.

4.2. Global nutrient circulation and phytoplankton distribution

There were only small seasonal variations along the 110°E meridian in the Indian Ocean sector of the Southern Ocean, compared with those in other areas in the Southern Ocean. The chl *a* concentration and phytoplankton composition differed among latitudinal zones. There were very low chl *a* levels around the SAZ (40–50°S). We size-fractionated cells collected in the different zones and found that micro-sized cells (>10 μm) were dominant in the southern regions. In other regions, pico-sized cells (0.7–2 μm) and nano-sized cells (2–10 μm) were generally more abundant (Fig. 4). From the results of phytoplankton pigment analysis, diatoms were more abundant in the micro-sized phytoplankton areas, and haptophytes were more abundant in the nano-sized phytoplankton areas (Fig. 5). Thus, the phytoplankton composition differed among the latitudinal zones in the Indian Ocean sector of Southern Ocean.

Nutrient distributions are important for phytoplankton composition. Diatoms are especially strongly affected by silicate concentrations and cannot grow with less than 10 μg m^{-3} silicate (Tsunogai, 1979; Tsunogai and Watanabe, 1983). Our vertical observation stations were at 5° latitude intervals, making it difficult to describe the vertical section of the 110° transect. So, we showed the WOCE cruise vertical

sections of nitrate, phosphate, and silicate concentrations along the 115°E transect (Fig. 7). All of the nutrients had higher concentrations at the southern stations. However, the ratio of change in concentration differed among the nutrients. In particular, nitrate and phosphate remained at higher levels while silicate was present at extremely low concentrations (<10 μg m^{-3}) in the northern regions. Silicate depletion has been recorded previously in this area. Various explanations have been proposed for the differences in decreasing ratios between phosphate and silicate in ocean waters. There are generally two explanations for the large-scale distribution of silicate within the Southern Ocean. The basic premises of both explanations are that (1) organic matter is remineralized at depths shallower than those at which dissolution of opal occurs, and (2) the downward shift in silicate relative to other nutrients is a result of global-scale biological productivity (Brocker and Peng, 1982; Dugdale et al., 1995). In other words, silicate becomes trapped in deep water circulation. Even if there is a high input of silicate to the surface, the preferential surface recycling of nutrients will lead to rapid preferential depletion of silicate (Dugdale et al., 1995). Sarmiento et al. (2004) proposed an alternative hypothesis based on preferential stripping of silicate in the Southern Ocean and low Si:N inputs into the upper ocean. Specifically, their alternative to the vertical trapping horizontal circulation mechanism proposed by Brocker and Peng (1982) is that silicate is present at high levels in the deep sea and low levels in the thermocline primarily because it is preferentially stripped from the deep waters of the Southern Ocean; thus, it cannot enter the main thermocline. They also emphasize the importance of the low Si:N ratio in supply waters in determining and limiting diatom production rather than the preferential recycling of nitrate as proposed by Dugdale et al. (1995).

Interestingly, most of the nitrate in the main thermocline is pre-formed; that is, except for a few regions (tropical Atlantic and Pacific, and north Pacific), the nitrate present in the thermocline is mainly derived from water that sinks from the ocean surface, rather than from remineralized organic matter. Considering this fact, the almost complete absence of silicate implies that there must be a very small amount of silicate in waters entering the main thermocline from the ocean surface. The only major region of the ocean surface with low silicate and high nitrate levels is a band between approximately 40°S and 60°S in the Southern Ocean. To understand these processes in the Southern Ocean, we first must understand the meridional overturning circulation pattern. The CDW upwells to the ocean surface at the Antarctic coast. The upper component of the CDW is carried north by wind-driven Ekman transport, where some of it sinks to form Antarctic Intermediate Water in the vicinity of the PFZ. More of it sinks to form Subantarctic Mode Water in the vicinity of the SAZ. The upwelling of deep waters and deep mixing in the SACCZ brings large amounts of nutrients to the surfaces of the ACC, AAZ, and PFZ. As Ekman transport carries these waters north, organisms use the nitrate, silicate, and other nutrients. However, the uptake of silicate is more efficient than that of nitrate, and consequently, the nitrate concentration remains high in a band where the silicate concentration is extremely low.

The preferential removal of silicate within the AAZ and PFZ is well-known (Kamykowski and Zentara, 1985; Pondaven et al., 2000; Smith et al., 2000. Brzezinski et al., 2001), and iron limitation is generally considered to explain the dramatic increase in the Si:N content of diatoms in this band (Brzeinski et al., 2003; Franck et al., 2000). In fact, a large diatom bloom was observed in the Atlantic Ocean sector of the Southern Ocean (Bathmann et al., 1997; Peeken, 1997). In the 6°W transect of the Atlantic Ocean sector of the Southern Ocean, the sub-surface water was rich in silicate (>20 μg m^{-3}); in fact, this concentration was twice that found in the Indian Ocean Sector of the Southern Ocean (Veth et al., 1997; Sarmiento et al., 2004). A recent study suggested that the production of Antarctic Bottom Water has decreased (e.g. Purkey and Johnson, 2012), reflecting the general slowing of overturning circulation on a decadal scale. As a result, there would be greater silicate depletion in the PFZ and SAZ. Euphausiids are abundant in the PFZ, where they mainly feed on diatoms (e.g. McLeod et al., 2010). Therefore, a reduction in the biomass of diatoms in these areas would have a negative effect on the euphausiids.

Our study revealed that phytoplankton biomass and composition change within the latitudinal zones along the 110°E meridian in the Indian Ocean sector of the Southern Ocean. The seasonal changes in this region were small compared with those at the Kerguelen Plateau due to a lack of downstream effects from there. The phytoplankton concentration and composition were relatively uniform in the same latitudinal zone at different time points; however, there was a small but distinct spring bloom along the 110°E meridian. Therefore, meridional observations on a fine spatial scale are important to assess phytoplankton variability in the Indian Ocean sector of the Southern Ocean. In

addition, only small variations are expected in the 110°E meridian because of its topography. In other words, the variations in phytoplankton in this region could be attributed to long-term climate change. We have been monitoring observations from JARE from the 1960s to the present. Our study revealed little seasonal variability in phytoplankton distributions and compositions in the same surface water masses. Thus, the JARE historical data can be used to evaluate the decadal changes of phytoplankton variability in the Indian Ocean sector of the Southern Ocean. In addition, the transect is near the WOCE I9 transect (115°E meridian), easing data comparisons between the two. We should continue to monitor the 110°E meridian in the future and to evaluate the effects of climate change on this ecosystem.

5. Conclusion

In this study, we identified the seasonal variations in phytoplankton biomass and species composition in the Indian Sector of the Southern Ocean using multi-ship, multi-seasonal observations. The chl *a* concentration was uniform within the same latitudinal zone at different time points, except during a small but distinct spring bloom that occurred north of 45°S and south of 60°S along the 110°E meridian. The phytoplankton species composition was also uniform within the same latitude zone at different time points from late spring to late summer. At the northern station, the phytoplankton community was dominated by haptophytes, and the ratio of diatoms increased further south. The paucity of dissolved iron may explain the low chl *a* concentration in this region. Iron upwells from the subsurface at the Kerguelen Plateau because of its topography. However, iron is depleted at the 110°E meridian. The difference in species composition among the latitudinal zones was because of differences in macronutrient distributions. Because of its short residence time, silicate is depleted in the PFZ; this is related to global nutrient circulation. We believe that monitoring the long-term variability of ecosystems in the Southern Ocean is important. The differences in phytoplankton abundance are relatively small compared with those in other, high-productivity areas. However, the long-term variations in this area should not be neglected, because they reflect the effects of global warming and climate change. Therefore, the 110°E meridian should continue to be monitored to evaluate the effects of climate change on this ecosystem. The establishment of a sentinel monitoring system in this area would be advantageous.

Acknowledgments

The authors thank Dr. Kunio T. Takahashi and Dr. Tomomi Takamura for collecting samples JARE53 and JARE54. We also thank the captains and crews of the *Umitaka-Maru* and *Shirase*, and many other colleagues on board for their assistance during the JARE and *Kaiyodai* Antarctic Research Expedition (*K*ARE) cruises. This study was supported by JSPS KAKENHI Grant Number, 23510019, 2011–2013 and NIPR research project KP-4. The production of this paper was supported by an NIPR publication subsidy.

References

Arrigo, K.R., Worthen, D., Schnell, A., Lizotte, M.P., 1998a. Primary production in Southern Ocean waters. J. Geophys. Res. 103, 15587–15600. http://dx.doi.org/10.1029/98JC00930.

Arrigo, K.R., Robinson, D.H., Worthen, D.L., Schieber, B., Lizotte, M.P., 1998b. Bio-optical properties of the southwestern Ross Sea. J. Geophys. Res. 103 (C10), 21683–21695.

Arrigo, K.R., van Dijken, G.L., Bushinsky, S., 2008. Primary production in the Southern Ocean, 1997–2006. J. Geophys. Res. 113, C08004. http://dx.doi.org/10.1029/2007JC004551.

Bathmann, U.V., Scharek, R., Klaas, C., Dubischar, C.D., Smetracek, V., 1997. Spring development of phytoplankton biomass and composition in major water masses of the Atlantic Sector of the Southern Ocean. Deep-Sea Res. II 44 (1–2), 51–67.

Belkin, I.M., Gordon, A.L., 1996. Southern Ocean fronts from the Greenwich meridian to Tasmania. J. Geophys. Res. 101 (C2), 3675–3696. http://dx.doi.org/10.1029/95JC02750.

Blain, S., Quéguiner, B., Armand, L., Belviso, S., Bombled, B., Bopp, L., Bowie, A., Brunet, C., Brussaard, C., Carlotti, F., Christaki, U., Corbière, A., Durand, I., Ebersbach, F., Fuda, J.-L., Garcia, N., Gerringa, L., Griffiths, B., Guigue, C., Guillerm, C., Jacquet, S., Jeandel, C., Laan, P., Lefèvre, D., Lo Monaco, C., Malits, A., Mosseri, J., Obernosterer, I., Park, Y.-H., Picheral, M., Pondaven, P., Remenyi, T., Sandroni, V., Sarthou, G., Savoye, N., Scouarnec, L., Souhaut, M., Thuiller, D., Timmermans, K., Trull, T., Uitz, J., van Beek, P., Veldhuis, M., Vincent, D., Viollier, E., Vong, L., Wagener, T., 2007. Effect of natural iron fertilization on carbon sequestration in the Southern Ocean. Nature 446, 1070–1074. http://dx.doi.org/10.1038/nature05700.

Blain, S., Sarthou, G., Laan, P., 2008. Distribution of dissolved iron during the natural iron-fertilization experiment KEOPS (Kerguelen Plateau, Southern Ocean). Deep-Sea Res. II 55, 594–605.

Boyd, P.W., Ellwood, M.J., 2010. The biogeochemical cycle of iron in the ocean. Nat. Geosci. 3 (10), 675–682. http://dx.doi.org/10.1038/ngeo964.

Brocker, W.S., Peng, T.H., 1982. Tracers in the Sea. Lamont-Doherty Geological Observatory, Palisades, New York.

Brzezinski, M.A., Nelson, D.M., Franck, V.M., Sigmon, D.E., 2001. Silicon dynamics within an intense open-ocean diatom bloom in the Pacific sector of the Southern Ocean. Deep- Sea Res. II 48, 3997–4018.

Brzezinski, M.A., Dickson, M.-L., Nelson, D.M., Sambrotto, R., 2003. Ratios of Si, C and N uptake by microplankton in the Southern Ocean. Deep-Sea Res. II 50, 619–633.

Comiso, J.C., McClain, C.R., Sullican, C.W., Ryan, J.P., Leonard, C.L., 1993. Coastal Zone Color Scanner pigment concentrations in the Southern Ocean and relationship to geophysical surface features. J. Geophys. Res. 98, 2419–2451. http://dx.doi.org/10.1029/92JC02505.

DiTullio, G.R., Grebmeier, J.M., Arrigo, K.R., Lizotte, M.P., Robinson, D.H., Leventer, A., Barry, J.P., VanWoert, M.L., Dunbar, R.B., 2000. Rapid and early export of Phaeocystis antarctica blooms in the Ross Sea, Antarctica. Nature 404, 595–598.

Dugdale, R.C., Wilkerson, F.P., Minas, H.J., 1995. The role of a silicate pump in driving new production. Deep-Sea Res. I 42, 697–720.

Franck, V.M., Brzezinski, M.A., Coale, K.H., Nelson, D.M., 2000. Iron and silicic acid concentrations regulate Si uptake north and south of the polar frontal zone in the Pacific Sector of the Southern Ocean. Deep-Sea Res. II 47, 3315–3338.

Gordon, A.L., Georgi, D.T., Taylor, H.W., 1977. Antarctic polar front zone in the Western Scotia sea-summer 1975. J. Phys. Oceanogr. 7, 309–328.

Hempel, G., 1985. Antarctic marine food web. In: Siegfried, W.R., Condy, P.R., Laws, R.M. (Eds.), Antarctic Nutrient Cycles and Food Webs. Springer, Berlin, pp. 266–270.

Iida, T., Mizobata, K., Saitoh, S.-I., 2012. Interannual variability of coccolithophore *Emiliania huxleyi* blooms in response to changes in water column stability in the eastern Bering Sea. Cont. Shelf Res. 34, 7–17.

Jeffrey, S.W., Wright, S.W., 1994. Photosynthetic pigments in the Haptophyta. In: Green, J.C., Leadbeater, B.S.C. (Eds.), The Haptophyte Algae. Clarendon Press, Oxford, p. 111.

Johnston, B.M., Gabric, A.J., 2010. Long-term trends in upper ocean structure and meridional circulation of the Southern Ocean south of Australia derived from the SODA reanalysis. Tellus A 62A, 719–736.

Johnston, B.M., Gabric, A.J., 2011. Interannual variability in estimated biological productivity in the Australian sector of the Southern Ocean in 1997–2007. Tellus B 63, 266–286.

Kamykowski, D., Zentara, S.-J., 1985. Nitrate and silicic acid in the world ocean: patterns and processes. Mar. Ecol. Prog. Ser. 26, 47–59.

Latasa, M., 2007. Improving estimations of phytoplankton class abundances using CHEMTAX. Mar. Ecol. Prog. Ser. 329, 13–21.

Latasa, M., Scharek, R., Vidal, M., Vila-Reixach, G., Gutiérrez-Rodríguez, A., Emelianov, M., Gasol, J., 2010. Preferences of phytoplankton groups for waters of different trophic status in the northwestern Mediterranean Sea. Mar. Ecol. Prog. Ser. 407, 27–42.

Li, F., Ginoux, P., Ramaswamy, V., 2008. Distribution, transport, and deposition of mineral dust in the Southern Ocean and Antarctica: contribution of major sources. J. Geophys. Res. 113, D10207. http://dx.doi.org/10.1029/2007JD009190.

Loeb, V., 2007. Environmental variability and the Antarctic marine ecosystem. In: Vasseur, D.A., McCann, K.S. (Eds.), The Impact of Environmental variability on Ecological Systems, The Peter Yodzis Fundamental Ecology Series, vol. 2, pp. 197–225.

Mackey, M.D., Mackey, D.J., Higgins, H.W., Wright, S.W., 1996. CHEMTAX – a program for estimating class abundances from chemical markers: application to HPLC measurements of phytoplankton. Mar. Ecol. Prog. Ser. 144, 265–283.

Martin, J.H., Gordon, R.M., Fitzwaters, S.E., 1990. Iron in Antarctic waters. Nature 345, 156–158.

Massom, R.A., Stammerjohn, S.E., 2010. Antarctic sea ice change and variability – physical and ecological implications. Polar Sci. 4, 149–186.

Massom, R.A., Reid, P., Stammerjohn, S., Raymond, B., Fraser, A., Ushio, S., 2013. Change and variability in East Antarctic sea ice seasonality, 1979/80–2009/10. PLoS One 8, e64756.

McLeod, D.J., Hosie, G.W., Kitchener, J.A., Takahashi, K.T., Hunt, B.P.V., 2010. Zooplankton Atlas of the Southern Ocean: the SCAR SO-CPR Survey (1991–2008). Polar Sci. 4, 353–385.

McNeil, B.I., Metzl, N., Key, R.M., Matear, R.J., Corbiere, A., 2007. An empirical estimate of the Southern Ocean air-sea CO_2 flux. Glob. Biogeochem. Cyl. 21, GB3011. http://dx.doi.org/10.1029/2007GB002991.

Mongin, M., Molina, E., Trull, T.W., 2008. Seasonality and scale of the Kerguelen plateau phytoplankton bloom: a remote sensing and modeling analysis of the influence of natural iron fertilization in the Southern Ocean. Deep-Sea Res. II 55, 880–892.

Montes-Hugo, M., Doney, S.C., Ducklow, H.W., Fraser, W., Martinson, D., Stammerjohn, S.E., Schofield, O., 2009. Recent changes in phytoplankton Western Antarctic Peninsula. Science 323, 1470–1473.

Moore, J.K., Abbott, M.R., 2000. Phytoplankton chlorophyll distributions and primary production in the Southern Ocean. J. Geophys. Res. 105, 28709–28722. http://dx.doi.org/10.1029/1999JC000043.

Nowlin Jr., W.D., Klinck, J.M., 1986. The physics of the Antarctic circumpolar current. Rev. Geophys. 24 (3), 469–491.

O'Reilly, J.E., Maritorena, E., Siegel, D.A., O'Brien, M.C., Toole, D., Mitchell, B.G., Kahru, M., Chavez, F.P., Strutton, P., Cota, G.F., Hooker, S.B., McClain, C.R., Carder, K.L., Muller-Karger, F., Harding, L., Magnuson, A., Phinney, D., Moore, G.F., Aiken, J., Arrigo, K.R., Letelier, R., Culver, M., 2000. In: Hooker, S.B., Firestone, E.R. (Eds.), SeaWiFS Post-launch Calibration and Validation Analyses, Part 3, NASA Tech. Memo. 2000-206892, vol. 11. NASA Goddard Space Flight Center, 49 pp.

Orsi, A.H., Whitworth, T., Nowlin Jr., W.D., 1995. On the meridional extent and fronts of the Antarctic circumpolar current. Deep-Sea Res. I 42 (5), 641–673.

Parsons, T.R., Maita, Y., Lalli, C.M., 1984. A manual of chemical and biological methods for seawater analysis, 1st ed. Fluorometric determination of chlorophylls. In: A manual of chemical and biological methods for seawater analysis, first ed. Pergamon Press Inc., New York, 14–17.

Peeken, I., 1997. Photosynthetic pigment fingerprints as indicators of phytoplankton biomass and development in different water masses of the Southern Ocean during austral spring. Deep-Sea Res. II 44 (1–2), 261–282.

Pondaven, P., Raqgueneau, O., Tréguer, P., Dezileau, L., Reyss, J.L., 2000. Resolving the 'opal paradox' in the Southern Ocean. Nature 405, 168–172.

Porra, R.J., Thompson, W.A., Kriedemann, P.E., 1989. Determination of accurate extinction coefficients and simultaneous equations for assaying chlorophylls a and b extracted with four different solvents: verification of the concentration of chlorophyll standards by atomic absorption spectroscopy. Biochim. Biophys. Acta (BBA) – Bioenerg. 975 (3), 384–394. http://dx.doi.org/10.1016/S0005-2728(89)80347-0.

Purkey, S.G., Johnson, G.C., 2012. Global contraction of Antarctic bottom water between the 1980s and 2000s*. J. Clim. 25, 5830–5844.

Rintoul, S.R., Bullister, J.L., 1999. A late winter hydrographic section from Tasmania to Antarctica. Deep-Sea Res. I 46, 1417–1454.

Sarmiento, J.L., Gruber, N., Brzezinski, M.A., Dunne, J.P., 2004. High latitude controls of the global nutricline and low latitude biological productivity. Nature 427, 56–60.

Smith, W.O., Anderson, R.F., Moore, J.K., Codispoti, L.A., Morrison, J.M., 2000. The U.S. Southern ocean joint global ocean flux study: an introduction to AESOPS. Deep-Sea Res. II 47, 3073–3093.

Sokolov, S., Rintoul, S.R., 2002. Structure of Southern Ocean fronts at 140°E. J. Mar. Sys. 37, 151–184.

Sokolov, S., Rintoul, S.R., 2007. On the relationship between fronts of the Antarctic circumpolar current and surface chlorophyll concentrations in the Southern Ocean. J. Geophys. Res. 112, 1–17.

Strutton, P.G., Gri, F.B., Waters, R.L., Wright, S.W., Bindo, N.L., 2000. Primary productivity off the coast of East Antarctica (80–150°E): January to March 1996. Deep-Sea Res. II 47, 2327–2362.

Suzuki, R., Ishimaru, T., 1990. An improved method for the determination of phytoplankton chlorophyll using N, N-dimethylformamide. J. Oceanogr. 46, 190–194.

Takahashi, T., Stewart, C., Sutherland, S.C., Wanninkhof, R., Sweeney, C., Feely, R.A., Chipman, D.W., Hales, B., Friederich, G., Chavez, F., Sabine, C., Watson, A., Bakker, D.C.E., Schuster, U., Metzl, N., Yoshikawa-Inoue, H., Ishii, M., Midorikawa, T., Nojiri, Y., Körtzinger, A., Steinhoff, T., Hoppema, M., Olafsson, J., Arnarson, T.S., Tilbrook, B., Johannessen, T., Olsen, A., Bellerby, R., Wong, C.S., Delille, B., Bates, N.R., Baar, H.J.W. De, 2009. Climatological mean and decadal change in surface ocean pCO_2, and net sea − air CO_2 flux over the global oceans. Deep-Sea Res. II 56 (8–10), 554–577.

Tilbrook, B., Rintoul, S., Watanabe, S., 2001. Carbon Dioxide, Hydrographic, and Chemical Data Obtained During the R/V Aurora Australis Repeat Hydrography Cruise in the Southern Ocean: CLIVAR Repeat Section I09S_2004. Carbon Dioxide Information Analysis Center, Oak Ridge National Laboratory, US Department of Energy, Oak Ridge, Tennessee. http://dx.doi.org/10.3334/CDIAC/OTG.CLIVAR_I09S_2004. http://cdiac.ornl.gov/ftp/oceans/CLIVAR/I09S_2004/.

Toggweiler, J.R., Russell, J., 2008. Ocean circulation in a warming climate. Nature 451 (7176), 286–288. http://dx.doi.org/10.1038/nature06590.

Tsunogai, S., 1979. Dissolved silica as a primary factor determining the composition of phytoplankton classes, in the ocean. Bull. Fac. Fish. Hokkaido Univ. 30, 314–322.

Tsunogai, S., Watanabe, 1983. Role of dissolved silicate in the occurrence of phytoplankton bloom. J. Oceanogr. Soc. Jpn. 39, 231–239.

Tynan, C.T., 1998. Ecological importance of the southern boundary of the Antarctic circumpolar current. Nature 392, 708–710. http://dx.doi.org/10.1038/33675.

Van Heukelem, L., Thomas, C.S., 2001. Computer-assisted high-performance liquid chromatography method development with applications to the isolation and analysis of phytoplankton pigments. J. Chromatogr. A 910 (1), 31–49.

Veth, C., Peeken, I., Scharek, P., 1997. Physical anatomy of fronts and surface waters in the ACC near the 6°W meridian during austral spring 1992. Deep-Sea Res. II 44 (1–2), 23–49.

Welschmeyer, N.A., 1994. Fluorometric analysis of chlorophyll chlorophyll b and pheopigments. Limnol. Oceanogr. 39, 1985–1992.

Wright, S.W., van den Enden, R.L., Pearce, I., Davidson, A.T., Scott, F.J., Westwood, K.J., 2010. Phytoplankton community structure and stocks in the Southern Ocean (30–80°E) determined by CHEMTAX analysis of HPLC pigment signatures. Deep-Sea Res. 57, 758–778.